TABLE II Values of Schmid factor in 12 shear directions for $[3\,2\,3]_A$ and $[2\,2\,3]_A$ tensile axes

Plane (A)	Shear direction [A]	Thompson tetrahedron notation	Values of Schmid factor in two tensile directions	
			[3 2 3]	[2 2 3]
$(\bar{1}\,1\,\bar{1})$	$[2\,1\,\bar{1}]$	Cα	−0.204	−0.124
	$[\bar{1}\,2\,\bar{1}]$	Dα	0.421	0.365
	$[\bar{1}\,1\,2]$	Bα	−0.217	−0.240
(1 1 1)	$[\bar{2}\,1\,1]$	Bδ	−0.066	−0.100
	$[1\,\bar{2}\,1]$	Aδ	0.159	0.081
	$[1\,1\,\bar{2}]$	Cδ	−0.093	−0.181
$(1\,\bar{1}\,\bar{1})$	$[2\,\bar{1}\,\bar{1}]$	Dβ	0.253	0.378
	$[1\,2\,\bar{1}]$	Cβ	−0.093	−0.133
	$[1\,\bar{1}\,2]$	Aβ	−0.161	−0.246
$(\bar{1}\,\bar{1}\,1)$	$[2\,\bar{1}\,1]$	Aγ	−0.143	−0.075
	$[\bar{1}\,2\,1]$	Bγ	−0.088	−0.077
	$[\bar{1}\,\bar{1}\,\bar{2}]$	Dγ	0.231	0.152

shows the values of Schmid factor in 12 shear directions for $[3\,2\,3]_A$ and $[2\,2\,3]_A$ tensile axes. As a shear direction with a maximum value of Schmid factor, Dα and Dβ are found for $[3\,2\,3]_A$ and $[2\,2\,3]_A$ tensile axes, respectively. In $[3\,2\,3]_A$ tensile axis, 1–5 and 1–6 variants contain Dα as a first shear and 3–6 and 4–4 contain Dβ as a second shear and 3–3 and 3–4 contain Dβ as a first shear in $[2\,2\,3]_A$ axis. As shown in Table I, 1–5 and 1–6 variants in $[3\,2\,3]_A$ and 3–3 and 3–4 variants in $[2\,2\,3]_A$, are formed by compression testing, and 4–4 variants in $[2\,2\,3]_A$ have the second largest value of U/σ. K–S variants obtained by Schmid factor do not necessary agree with those which are obtained by the U/σ calculation. Then, by discussing K–S variants obtained from two methods, 3–6 variant in $[3\,2\,3]_A$ and 1–3 variant in $[2\,2\,3]_A$ are selected as the variants which agree each other. Finally, calculating both the interaction of applied stress with displacive shear during martensite transformation and possible Kurdjumov–Sachs variants in relation to the double shear process, Kurdjumov–Sachs variants induced by tensile deformation were obtained (Table II).

References

1. R. LAGNEBORG, *Acta Met.* **12** (1964) 823.
2. D.GOODCHILD, W.T. ROBERTS and D.V. WILSON, *ibid.* **18** (1970) 1137.
3. T. NAKAMURA and K. WAKASA, *Scripta Met.* **9** (1975) 959.
4. K. WAKASA and T. NAKAMURA, *J. Mater. Sci.* **13** (1978) 21.
5. J. R. PATEL and M. COHEN, *Acta Met.* **1** (1953) 531.
6. M. KATO and T. MORI, *ibid.* **24** (1976) 853.
7. A. J. BOGERS and W. G. BURGERS, *ibid.* **12** (1964) 225.
8. Y. HIGO, F. LECROISEY and T. MORI, *ibid.* **22** (1974) 313.

Received 22 December 1977
and accepted 10 March 1978.

KUNIO WAKASA*
Institute for Medical and Dental Engineering,
Tokyo Medical and Dental University,
2-3-10 Surugadai,
Kanda, Chiyoda-ku,
Tokyo, Japan
TADAHISA NAKAMURA
Department of Materials Science and Engineering,
Tokyo Institute of Technology,
O-okayama, Meguro-ku,
Tokyo, Japan

*Now at: Department of Metallurgy and Mining Engineering, University of Illinois at Urbana, Champaign, Urbana, Illinois 61801, USA.

Explosive-shock deformation of natural chalcopyrite ($CuFeS_2$)

The authors recently described the defect structure in natural chalcopyrite utilizing transmission electron microscopy [1]. On the basis of these observations, it was concluded that the apparently low stacking-fault free energy in $CuFeS_2$ which was deduced from numerous observations of stacking faults, would give rise to abundant mechanical twins accommodating large deformations. It was assumed in fact, that large numbers of stacking faults and twin faults might form in response to large deformation such as explosive-shock deformation as in the case of f c c metals and alloys and other minerals [2–5].

The present study involved an experiment to test this prediction. A whole section of natural

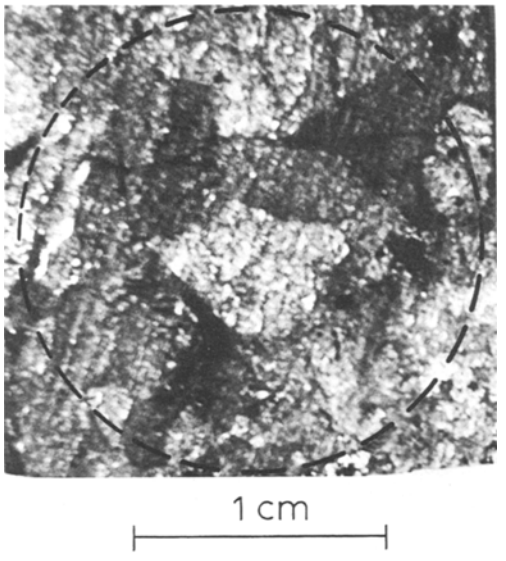

Figure 1 Example of chalcopyrite test wafer from which cylindrical specimen was prepared for shock deformation. Large grain size is apparent. The dotted circle approximates the diameter of the final test specimen.

(polycrystalline) chalcopyrite was deformed by explosive-shock loading and the residual microstructures observed by transmission electron microscopy.

A technique similar to but modified from that outlined previously by Rose and Grace [6] and Murr and Grace [7] was employed in the shock experiment. Several pieces of natural (Transvaal, South Africa) chalcopyrite were cut and polished to roughly 19 mm square and 3.5 mm thick as shown typically in Fig. 1. A circular piece was then shaped from these pieces as shown dotted in

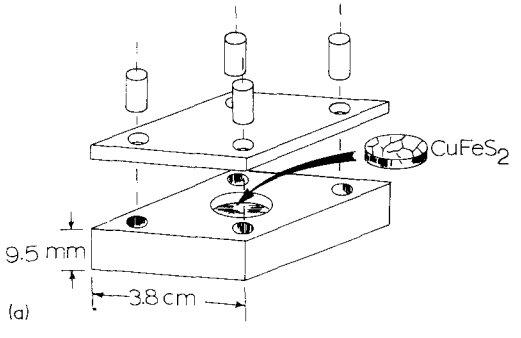

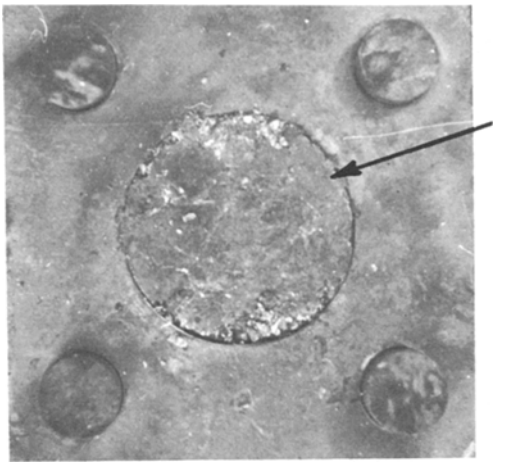

Figure 3 Experimental shock sandwich recovered from water recovery tank. The bottom portion containing the chalcopyrite cylinder in sandwich base (arrow) is shown.

Fig. 1. While several attempts were made, only one final circular sample was utilized in the shock assembly. The shock loading assembly was made from a Ti–6Al–4V alloy having a nearly compatible density of 4.4 g cm^{-3} as compared to a density of 4.3 g cm^{-3} measured for the chalcopyrite test pieces. This was necessary in order to

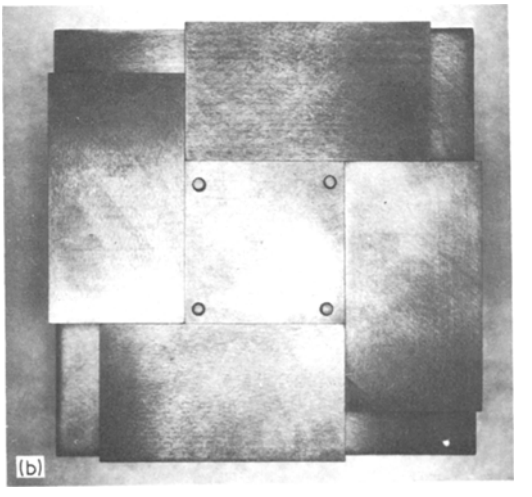

Figure 2 Experimental shock-loading sandwich and assembly. (a) Ti–6Al–4V Sandwich assembly. The cyclindrical $CuFeS_2$ sample was pressed into the sandwich base and small void spaces around the perimeter filled with powdered chalcopyrite mixed with an acetone-base glue. (b) Sandwich in (a) was pinned and machined to 16 μm surface finish, placed on a 25 mm thick Ti-alloy spall plate (measuring 10.16 cm square), and Ti-alloy momentum pieces positioned around the sandwich perimeter as shown.

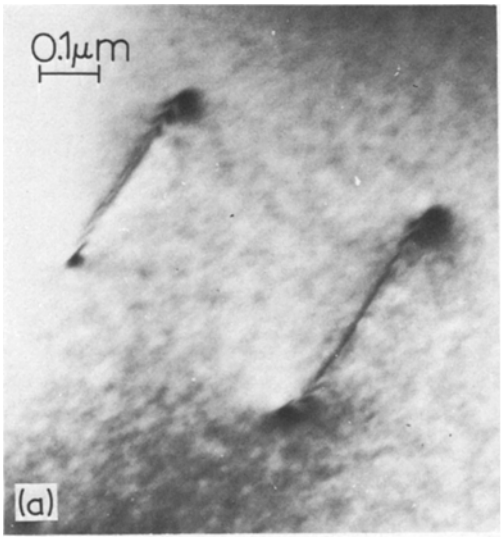

Figure 4 Comparison of unshocked and shocked chalcopyrite microstructure. (a) Bright-field transmission electron micrograph showing dislocations in unshocked chalcopyrite. The dislocation density evident in the micrograph is typical of the unshocked material. (b) Bright-field image showing dislocations and twin-faults in unshocked chalcopyrite. (c) Heavily dislocated portion of shock-loaded chalcopyrite typical of the residual, shocked microstructure.

eliminate shock rarefaction effects which would contribute to the pulverizing of the chalcopyrite sample. A Ti-alloy sandwich was made to contain the chalcopyrite test piece by machining a snug-fit hole in a base section as illustrated in Fig. 2a. A 3 mm thick cover plate was then pinned to the base piece using 6.25 mm diameter Ti-alloy dowel pins. The sandwich containing the chalcopyrite cylinder was then placed on a 25 mm thick spall plate and momentum-trap pieces placed around the sandwich as shown in Fig. 2b. A 0.49 cm thick 304 stainless steel flyer plate was used to impact the assembly surface shown in the illustration in Fig. 2b. This thickness was calculated to give a pulse duration of roughly 2 μsec. A duPont Detasheet C-4 line-wave generator was used as the only explosive. The flyer–plate standoff distance was approximately 20 mm. The sandwich was recovered intact in a 2 m-deep water recovery tank following the explosive-test event.

By interpolating a Rankine-Hugoniot curve for the Ti–6Al–4V alloy from aluminium and titanium Hugoniot curves [6] and using the interpolated curve along with the Hugoniot for 304 stainless steel in the impedance-matching technique [7, 8], the peak shock pressure in the chalcopyrite was determined to be 19 GPa (190 kbars).

The reason for utilizing the shock deformation arrangement described above was that this seemed to be the only method of inducing large deformations in the chalcopyrite while keeping the test material relatively intact. This would insure the formation of defects in relatively large pieces which could be broken into small shards or chips for examination in the electron microscope, and insure that the majority of defects present would not be induced by the process of forming the chips.

Electron-transparent sections of the chalcopyrite test sample were prepared by crushing or chipping larger pieces of the recovered, shocked material. Small, flat chips were placed between two 200 mesh electron microscope screen grids using a vacuum tweezer and observed in a Hitachi Perkin–Elmer H.U. 200 F transmission electron microscope operating at 200 kV, employing a goniometer tilt stage.

Fig. 3 shows the shocked, recovered sandwich containing the cylindrical chalcopyrite test specimen. It can be noted that while some fragmentation has occurred, there remain numerous, large pieces, usually the size of individual grains (~2 to 4 mm).

Fig. 4 shows for comparison several examples of the chalcopyrite before and after shock deformation. Fig. 4a depicts the average dislocation density in the unshocked chalcopyrite, while Fig. 4b illustrates the presence of stacking faults or twin faults in the unshocked material. Fig. 4c shows a typical view of the dislocation structure in the shocked chalcopyrite. There was, as depicted in Fig. 4c no evidence of shock-induced stacking faults or twin faults.

The dislocation density measured in the unshocked material was $3(\pm 1) \times 10^7$ cm^{-2}. Correspondingly, the dislocation density in the shocked chalcopyrite was measured to be approximately $6(\pm 2) \times 10^{10}$ cm^{-2}. The method of Ham [9] was used in making the dislocation density measurements, and the necessary film thickness was determined by counting extinction fringes at faults (as in Fig. 4b), or at diffraction contrast fringes at the edge of the foil and estimating the thickness by calculating the extinction distance from fault projections having the same operating reflection [10].

Fig. 5 shows for comparison X-ray powder patterns for the unshocked and shock-loaded chalcopyrite. There is no evidence of any shock-induced transformation. There is, however, a consistent broadening of the diffraction lines for the shock-loaded chalcopyrite, consistent with the differences in the dislocation density as noted above.

In view of the observations of shock-loaded chalcopyrite (Fig. 4c) it is apparent that, contrary to what has been suggested previously [1], the stacking-fault free energy is relatively high, and chalcopyrite does not twin readily if at all in response to large deformations. This may be indicative that the faults observed in the undeformed chalcopyrite (Fig. 4b) are growth faults of some kind.

The present study points up a need to evaluate more critically the residual structure (defect

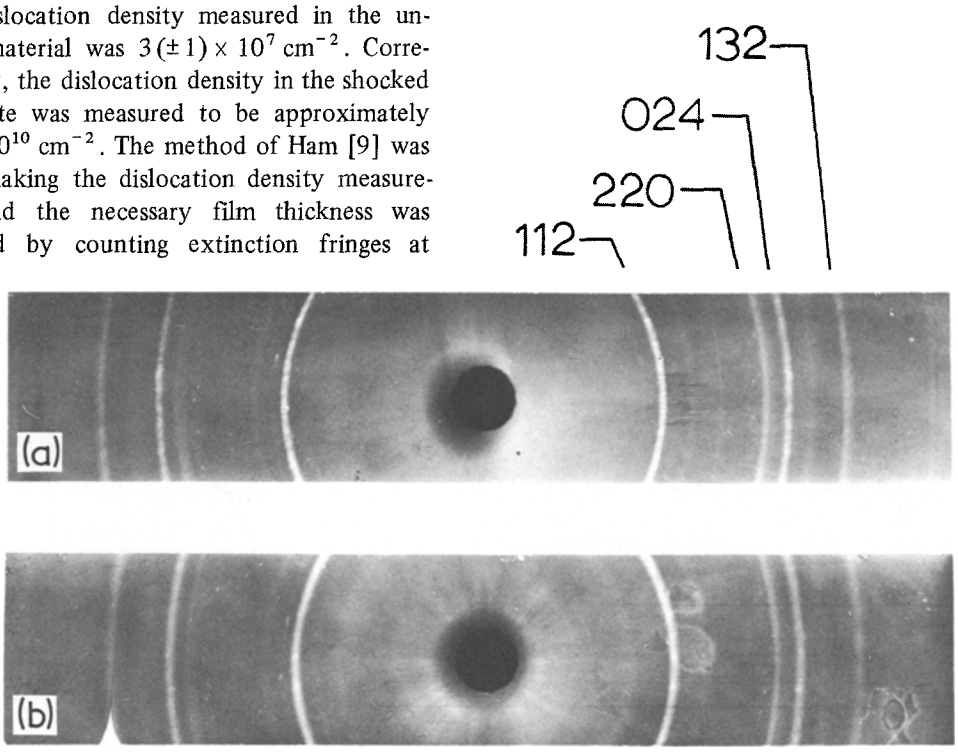

Figure 5 X-ray powder patterns for (a) unshocked and (b) explosive shock-loaded chalcopyrite.

structure) in deformed chalcopyrite compounds. While no abundant mechanical twins as predicted have been observed in shock-deformed natural chalcopyrite, large numbers of dislocations have been observed as noted in Fig. 4c. It is not unlikely, therefore, that certain grinding techniques could also induce large numbers of dislocations which would have an effect on the kinetics of chalcopyrite concentrate leaching. This feature is in fact being tested and the results will be reported elsewhere.

Natural chalcopyrite shock-loaded to a pressure of 19 GPa (190 kbars) was observed to form roughly 10^3 times more dislocations than present in the unshocked material. There was, contrary to previous predictions [1], no evidence of shock-induced faulting or mechanical twins leading to the conclusion that faults observed in the unshocked chalcopyrite arise by growth phenomena. There was no evidence of a shock-induced phase transformation.

Acknowledgements

This research was supported in part by a National Science Foundation (RANN) Grant (AER-76-03758-A01) through the John D. Sullivan Center for *In Situ* Mining Research. One of us (SLL) wishes to acknowledge support through a Battelle–Sullivan Fellowship.

References

1. L. E. MURR and SUZANNE L. LERNER, *J. Mater. Sci.* 12 (1977) 1349.
2. L. E. MURR and F. I. GRACE, *Exptl. Mech.* 9 (1969) 145.
3. L. E. MURR and K. P. STAUDHAMMER, *Mater. Sci. Eng.* 20 (1975) 35.
4. "Electron Microscopy in Mineralogy", edited by H.-R. Wenk, P. E. Champness, J. M. Christy, J. M. Cowley, A. H. Heuer, G. Thomas and N. J. Tighe (Springer Verlag, New York, 1976).
5. "Metallurgical Effects at High Strain Rates", edited by R. W. Rohde, B. M. Butcher, J. R. Holland and C. H. Karnes (Plenum Press, New York, 1973).
6. R. G. McQUEEN, E. G. ZUKAS and S. P. MARSH, "High-Velocity Impact Phenomena", edited by R. Kinslow (Academic press, New York, 1970) pp. 293, 515.
7. G. E. DIETER, "Response of Metals to High Velocity Deformation", edited by P. G. Shewmon and V. F. Zackay (Interscience, New York, 1961) p. 409.
8. G. E. DUVALL and G. R. FOWLES, "High Pressure Physics and Chemistry", Vol. 2, edited by R. S. Bradley (McGraw–Hill, New York, 1963) p. 209.
9. R. K. HAM, *Phil. Mag.* 6 (1961) 1183.
10. L. E. MURR, "Electron Optical Applications in Materials Science" (McGraw–Hill, New York, 1970).

Received 22 December 1977
and accepted 24 February 1978.

L. E. MURR
SUZANNE L. LERNER
Department of Metallurgical and Materials Engineering,
New Mexico Institute of Mining and Technology,
Socorro, New Mexico, USA

The growth of $Dy_3Al_5O_{12}$

Cockayne *et al.* [1] have grown DyAG ($Dy_3Al_5O_{12}$) single crystals by the Czochralski method. They reported that DyAG was the only rare earth aluminium garnet which grew with a flat interface even at rotation rates as low as 5 r.p.m. These workers also showed that a substantial portion of the radiation emitted by a DyAG melt was absorbed by the crystal and that, in consequence, low radial gradients were produced near the growing interface. Under such conditions, controlled growth of large diameter crystals is difficult.

In the present work, single crystals of DyAG have also been grown from stoichiometric melts by the Czochralski technique. The apparatus used for this experiment was made by Kokusai Electric Co. for oxide crystals. It has been modified for automatic diameter control (ADC). The ADC method adapted was a popular crystal weighing system and either analogue or digital control could be selected. The load cell which was used to weigh the crystal was made by Ohkura Electric Co. and had a high sensitivity (0.01 g). A simplified block diagram of this system is shown in Fig. 1.

In order to maintain a temperature gradient sufficiently steep for growth to be induced the